

1805

7.3

ОБЪЕДИНЕННЫЙ  
ИНСТИТУТ  
ЯДЕРНЫХ  
ИССЛЕДОВАНИЙ



JOINT  
INSTITUTE  
FOR NUCLEAR  
RESEARCH

Москва, Главпочтамт п/я 79

Head Post Office, P.O. Box 79, Moscow USSR

МЕЖДУНАРОДНАЯ КОНФЕРЕНЦИЯ ПО ФИЗИКЕ ВЫСОКИХ ЭНЕРГИЙ  
Дубна 5-15 августа 1964 г.

THE 1964 INTERNATIONAL CONFERENCE ON HIGH ENERGY PHYSICS

Dubna, August 5-15.

ДОКЛАДЫ РАППОРТЕРОВ RAPPOORTEURS' REVIEWS

E-1805

SEPARATION METHODS FOR HIGH  
AND SUPERHIGH ENERGY PARTICLES

Rapporteur M. Deusch

Secretary V.V. Miller

Дубна 1964

SEPARATION METHODS FOR HIGH  
AND SUPERHIGH ENERGY PARTICLES

Rapporteur M. Deusch

Secretary V.V. Miller

E-1805

2598/2 48.

**This publication is of a preliminary character.  
To facilitate the rapid appearance of Reports, they  
are printed in the form as presented by Rapporteurs.**

## Separated Beams

Both the 1962 CERN conference<sup>1)</sup> and the 1963 Dubna conference<sup>2)</sup> on accelerator instrumentation heard a considerable number of reports on separated particle beams. This has been a year of consolidation and I do not have any **important** developments to report. A number of new beams are described in communications to this conference and I shall try presently to summarise their most important features as examples of the current state of the art.

### Operating Experience

Of the several CERN beams described previously, the latest one, the so-called O2 beam (ref. 2, p. 782) was put into operation in February of this year, using the electrostatic separating system for 6 GeV/c  $K^-$  particles. Since the British National Bubble Chamber for which it was designed is not yet in operation it was used with some modification during June to obtain 260.000 pictures in the French chamber. It follows closely the expected performance.

An illustration of the utilization of separated beams is provided by the history of the CERN M2 beam, which was operated during the year 1963 to obtain 1 million bubble chamber pictures with  $K^+$  and  $K^-$  particles of 3.0 and 3.5 GeV/c, about 300.000 pictures of 5.2 GeV/c antiprotons and 200.000 pictures of  $\pi^+$  in deuterium. In addition it was used in a counter experiment on antiproton annihilation, giving about 1.000  $\bar{p}$  per  $10^{11}$  particles at 2.5 GeV/c.

This beam has now been dismantled and is to be replaced in April 1965 by a new short  $K^-$  beam consisting of a single stage of

separation, using considerably higher electric field strength than used.

During a comparable period a similar beam produced 500,000 pictures as the  $K^-$  particles and 750,000 pictures with  $\pi^-$  particles in the Berkeley 72 inch hydrogen bubble chamber.

#### Electrostatic Separators

Most electrostatic separators operate with field strengths of 50-70 kv/cm.

Experience in Berkeley has shown that glass-covered electrodes permit stable operation up to 100 kv/cm or even higher. Very recently it has been found at CERN that equally good or even better results can be obtained with aluminium covered with an insulating oxide layer by an ordinary anodizing procedure. A model gap has been tested for several weeks with a cathode of this construction and a stainless-steel anode with very satisfactory results.

#### Radiofrequency Separators

The tow-cavity r.f. separator for the CERN O2 beam mentioned previously has undergone some initial tests: one cavity has been powered to about 10 MW and beam deflection has been observed.

The radiofrequency separator for the 5 GeV/c Dubna antiproton beam (ref. 2 p. 788) is at approximately the same stage of development.

There have been no other reports of progress in radiofrequency systems but Valdner et al from Moscow<sup>3)</sup> have submitted a careful analysis of various types of wave-guide separators.

#### Some New Separated Beams

Two new beams, recently put into operation at the Berkeley

Bevatron are described in communications to this conference. The first of these, described by Murray et al.<sup>4)</sup> has been used for 2.5 + 2.8 BeV/c  $K^-$  particles with the 72 inch hydrogen bubble chamber. It has as its main feature a particularly through compensation of chromatic aberration, permitting acceptance of a momentum interval  $\Delta p/p = 0.04$ , with good separation. This achromatisation is achieved by producing a simultaneous stigmatic focus at the center line of the mass slit for all momenta in the accepted interval. The mass slit is oriented in the horizontal plane at a small angle with the optic axis (Z-direction) determined essentially by the ratio of the lateral momentum dispersion to the longitudinal chromatic aberration.

Table I shows the pertinent parameters for the beam described. The angles between the coordinate axes and the intersections of the slit jaws with the coordinate planes are denoted by  $\theta_s$  (horizontal angle with z-axis),  $\phi_s$  (vertical angle with z-axis),  $\psi_s$  (angle with x-axis in x-y plane). Z is the beam direction and x is vertical,  $g_o$  is the horizontal dispersion, in lowest order,  $\theta_m, \phi_m$  are the acceptance angles.

Note that the mass slits are almost parallel to the z-direction. The angle  $\psi_s$  is very nearly the angle of the slit jaw face. This is necessarily much smaller than in the case of a perpendicular slit orientation making the effective thickness of the jaws near the aperture correspondingly smaller.

Fig. 1 shows the beam transport system. It is representative of a current two-stage electrostatic separation system except for the singlet quadrupole lenses O6 and O11 which are required to assure stigmatism of the vertical and horizontal images, over the entire momentum band. The second separated beam at Berkeley

bevatron which has been described<sup>5)</sup> makes use of the extracted proton beam. This has several obvious advantages. The secondary particles can be produced at any desired angle with respect to the proton beam, including  $0^\circ$ , as is done in this particular arrangement. Since the particles do not traverse the fringe field of the accelerator, either positive or negative beams can be used and there is no difficulty in selecting any momentum band in a wide range,  $800 < p < 1600$  MeV/c in this case. Finally, the target is very accessible so that, in principle, a large solid angle may be achieved with moderately sized magnets provided sufficient care is taken to reduce aberrations. The beam lay-out is illustrated in Fig. 2. The position of the principal planes of the objective triplet  $Q_1$   $Q_2$   $Q_3$  can be changed by reversing the field in the two quadrupoles  $Q_2$  and  $Q_3$ , thus changing the magnification of the first stage of the system. For low momenta, large magnification is used, yielding larger acceptance and less favourable geometric resolution. For high momenta, the reverse condition is chosen. Ray diagrams for two modes of operation are shown, respectively in Fig. 3.

Chromatic aberration is compensated to some extent in the first stage by arranging the jaws of slit 1 to follow a line inclined at  $20^\circ$  with the beam direction which is the focus of vertical foci. In the second stage chromatic aberration is partly compensated by a sextupole component in M3 so that S2 is normal to the beam. This is important since there is no horizontal focus at this point.

The optical characteristics of this beam are summarised in Table II. Fig. 4 shows the yields of various particles per msterad for  $10^{11}$  extracted proton for 1% momentum spread.

The external target only intercepts 60 percent of the extracted beam. The separation obtained at 1600 MeV/c is illustrated in Fig. 5. The pion contamination of the  $K^+$  beam varies from about 1% at 860 MeV/c to about 20% at 1.6 GeV/c.

One of two electrostatically separated beams of the Dubna synchrophasotron has been put into operation and has been described by Vovenko et al.<sup>(6)</sup> in a communication to this conference. It is designed for positive particles up to 2.4 GeV/c and negative was up to 2.7 GeV/c, impinging on the 55 liter hydrogen bubble chamber located just outside the shielding wall, 43 m from the internal machine target, as illustrated in Fig. 6. The very restricted space available imposed special limitations on the design. For example the first deflection magnet, which imparts only  $4.5^\circ$  deflection has to be pulsed at the end of the acceleration cycle to prevent interference with machine operation.

Two electrostatic separators of 11 m length are used with a field of 55 kv/cm. Positive particles are taken at about  $19^\circ$  from the primary beam, negative particles near  $0^\circ$ . At 2 GeV/c the  $K^+$  separation is about 12 mm with a full width at half-intensity of the target image of about 7 mm. Under these conditions 8  $K^+$  particles and 1.5 relativistic background particles are obtained per  $10^{11}$  protons. Vertical and horizontal beam traces are illustrated in Fig. 7. The objective lens triplet can be adjusted to change the acceptance and separation characteristics of the system by changing the magnification. The lens  $\mathcal{N}_4$  located near the vertical focus of the objective provides compensation for horizontal dispersion in the deflection magnet



M<sub>2</sub>. The doublet  $\mathcal{M}_5, \mathcal{M}_6$  forms the slowly converging beam passing through the separators. A sextupole is placed at the momentum slit to provide a chromaticization but little improvement is obtained since the momentum dispersion in horizontal plane is not much greater than the target image size. A small vertically defocusing lens after the mass slit spreads the beam into a more desirable shape for the bubble chamber.

A new 6 GeV/c mass-separated beam at the ZGS in the Argonne laboratory has been described by Ammar et al<sup>7)</sup>. The main features of this system are the very symmetric arrangement of the optical elements and the use of an octupole corrector between the elements of each quadrupole doublet to correct fringing-field aberrations.

The horizontal field of the octupole is of the form  $B_x = k(12x^2y - 4y^3)$ . On the other hand the aberrational vertical momentum imparted by the fringe field is of the form  $p_y = k'x^2y$ . Compensation by an octupole is thus useful provided the vertical spread of the beam is much smaller than the horizontal spread, so that the  $y^3$  term can be neglected. Chromatic compensation is achieved by sextupole magnets. We have no description of the actual effectiveness of these higher multipole compensating magnets in a beam of small aperture.

The optical system is illustrated in Fig. 8. The first quadrupole pair produces a vertically parallel beam while forming a horizontal image of the source at the momentum slit. The second pair produces a vertical image of the target and a horizontal image of the momentum source point at the mass slit.

One new CERN beam which has been presented to this conference

achieves even higher acceptance without using an extracted beam.

It is somewhat different in conception from the other beams described. It is intended - and, in fact has been used - for counter spark chamber experiments rather than a bubble chamber. The experimental detection provides resolution in time as well as in space. Very large numbers of particle per machine pulse can therefore be used, provided the spill time can be made long enough. At the same time the entire burden of the separation need not be carried by the spatial separation provided by the electromagnetic separator since the transmitted particle can be further identified by usual counter techniques. The beam, as presently constituted, is more properly characterised as an enriched rather than a separated beam, since the background of pions is still 3.5 times as high as the transmitted antiproton beam. On the other hand the aperture at the entrance to the beam transport system is  $\sim 0.8 \cdot 10^{-3}$  steradian and particles are accepted at an angle of only  $6.3^\circ$  from the direction of the circulating proton beam hitting an internal target. This is achieved by a special design of the initial elements of the beam optics (see Fig. 9). The first bending magnet is located with its gap inside the accelerator chamber. The beam is carried through a beam pipe connected directly with the accelerator vacuum through the objective doublet  $Q_1, Q_2$ . These quadrupoles are of special construction, utilizing iron only in the return yoke and are designed for particularly large acceptance. The ability to design an accurate field shape is bought at the expense of a very high power consumption. Each quadrupole typically consumes 250 kw for a gradient of 700 Gauss/cm over 1 meter. The rest of the beam optics is rather conventional. The electrostatic

separator is 10 meters long and operates normally with about 50 kv/cm. Provision is made for two experimental stations, a very short  $K^-$  beam transport and a longer  $\bar{p}$  channel. The optics of the  $K^-$  beam is shown schematically in fig. 12. The doublet  $Q_3, Q_4$  acts as field lens, imaging the source on the experimental target over the entire accepted momentum range. No sextupole compensation for chromatic aberration is provided.

In the  $\bar{p}$  channel, about  $10^5 \bar{p}$  per machine pulse of  $10^{12}$  protons are obtained at 2.5 GeV/c ( $\pm 2\%$ ) with a 250 msec machine spill with a  $\pi^-$  background which is about 3.5 times as high. This peak intensity still permits easy identification of each particle by electronic detection with negligible accidental rates. If this beam were allowed to traverse a spark chamber directly one could obtain about 1 or 2 background tracks per picture for typical operating regimes. The  $K^-$  channel yields about  $4 \times 10^4 K^-$  burst with a pion background comparable in absolute number to that in the antiproton channel.

It is probable that high intensity beams will be of importance in the future as more complicated processes are studied in detail.

#### Very High Intensity Beams

We have had no communications concerning the operation of very high intensity meson beams of interest for neutrino experiments. A magnetic horn of improved design is approaching completion at the Z.G.S. Argonne laboratory. An interesting suggestion has been made by Vladimirovsky and Tarasov<sup>(9)</sup>. It is illustrated in Fig. 10. A magnetic mirror forming part of an ellipsoid of revolution focuses mesons originating at the target onto the neutrino detector. This system would have the advantage that the detector would not be in the direct line of the high intensity beam of

unwanted energetic neutrinos and gamma ray quanta. The authors estimate that a magnetic field of 15 kG (15 m long, 1 m wide and less than 30cm deep would be sufficient to focus mesons up to 10 GeV/c in a detector 100 m from the target.

### Magnetic Analysis

Two papers included in our session dealt with magnetic analysis for secondary particles, which are more properly part of detection rather than beam transport systems. Panofsky et al<sup>(10)</sup> propose an ingenious scheme to simplify the problem of analysing simultaneously the production angle and momentum of particles originating from a line target. Conventionally this is done by displaying the angular information horizontally and deflecting the particles vertically for momentum analysis. In the proposed device the momentum dispersion is horizontal simplifying the construction. The horizontal production angle is displayed vertically, while the horizontal deflection depends both on angle and momentum. An example of this concept is shown in Fig. 11. The line target is focused horizontally on the quadrupole  $Q_2$ . This intermediate image is then focused by  $Q_3$  on the image plane as well as by the bending magnets  $M_1$  and  $M_2$ . The horizontal positions of the focus in  $Q_2$  depend on the production angle. Hence the final position  $x_f$  depends both on  $\theta$  and  $\Delta p/p_0$ .  $Q_2$  does not affect the horizontal optics in first order, but if  $Q_2$  is rotated around the beam direction, there will be a vertical deflection proportional to the horizontal displacement at  $Q_2$  and hence to the production angle  $\theta$ . The position of the image point  $(x_f, y_f)$  thus uniquely determines both momentum and production angle. Note that only the rotated quadrupole is characteristic of this device. The rest of the optics may take many forms. For comparison we show

the optics of a spectrometer with vertical deflection Fig. 12 of comparable performance. Table III is an illustration of the kind of system contemplated by Panofsky and coworkers.

#### Monoenergetic Gamma ray Beams

More or less monoenergetic gamma rays have been produced from high-energy electron accelerators by three methods:

1. Coherent production from crystals.
2. Annihilation of secondary monoenergetic positrons.
3. Electronic selection of the gamma ray energy by measuring the energy remaining with the electron. (Tagging).

Only one paper submitted to this meeting deals with these problems.

(11)

Ballam & Guiragossian have calculated conditions for producing a highly monoenergetic beam ( $\Delta k/k \simeq 0.01$ ) of intensity suitable for bubble chamber operation from the SIAC electron accelerator.

It is proposed to produce positrons from a target after the first third of the accelerator and to accelerate these to about 15 GeV in the remaining sections. The annihilation quanta should then be accepted at an angle of about 10 mrad in a narrow angular range. This angle is determined by noting that the intensity of annihilation radiation drops linearly with angle while the most serious competing process, bremsstrahlung, drops as the cube of the angle. One therefore wants to operate at the largest angle consistent with acceptable energy and intensity. Very sharp collimation and a very thin target would be needed.

A contribution by K.D. Tolstov<sup>(12)</sup> addresses itself to the question of a hydrogen target inside the accelerator chamber. He

analyses the possibility of injecting a jet of liquid or solid hydrogen into the beam at the end of the acceleration cycle. Such a target would have the advantage of very low density, permitting multiple traversals but it would pose problems of stability and of absolute calibration.

It may be of interest in this connection, that the electron scattering group at the Cambridge Electron Accelerator has recently found very satisfactory solutions for the construction of internal liquid hydrogen targets made of thin plastic bags.

A communication by L.W. Jones<sup>(13)</sup> calls attention to the fact that useful focusing effects can be obtained by suitable arrangements of diffuse scatterers, especially in the case of neutral particles for which no convenient coherent focusing methods are available. The phenomenon used is the well known "scattering-in" which causes difficulty in absorption experiments: Any scattering material located in a part of the beam which would normally not reach the detector increases the flux. In the case of multiple coulomb scattering a simple, approximate analysis shows that, for cylindrical geometry, the scatterer should always have the thickness which places the detector at the root-mean-square scattering angle. Since the latter is proportional to the square of the thickness of the scatterer, a "scattering-in" lens should have parabolic cross-section, as illustrated in fig. 13. The lens radius is limited by the maximum thickness permissible without affecting the characteristics of the scattered particles too much. For example, with proton of 12.1 GeV/c a 1 cm "focal spot" can be obtained, 4.3 m from a lead "lens" of 10 cm radius with an enhancement of  $\phi = 2.45 \phi_0$ . Fig. 14 illustrates this focusing ef-

fect. This scheme may be useful for  $M$  meson beams in which large amounts of absorbing material are used.

The conditions for neutral particles are of course different and no detailed evaluation of the possibilities have yet been made.

Table I.

Values of various parameters pertinent to the "tilted mass slit" method of achromatization used in the K-63 separated  $K^-$  beam

Parameter	First stage	Second stage
$\phi_m$	$2.7 \cdot 10^{-3}$ rad.	$3 \cdot 10^{-3}$ rad.
$\theta_m$	$9 \cdot 10^{-3}$ rad.	$8 \cdot 10^{-3}$ rad.
$M_v$	-0.9	-0.9
$M_H$	-1.1	-1.1
$g_0$	0.5 in/%	0.5 in/%
$g_0 \cot \theta_s$	10 in/%	20 in/%
$\theta_s$	$50 \cdot 10^{-3}$ rad	$25 \cdot 10^{-3}$ rad
$\phi_s$	$3.3 \cdot 10^{-3}$ rad	$4.4 \cdot 10^{-3}$ rad
$\chi_s$	$65 \cdot 10^{-3}$ rad.	$176 \cdot 10^{-3}$ rad

Table II

Optical characteristics of the beam

	Mode I	Mode II
Momentum (MeV/c)	800-1200	1200-1600
Solid Angle (msr)	0.89	0.36
Length (target to chamber, inches)	1115	1115
Horizontal Acceptance Angle (mrad)	130	96
Vertical Acceptance Angle (mrad)	6.8	3.8
Total Momentum Bite	2%	1.5%
Vertical Magnification, First Stage	0.59	0.33
Horizontal Magnification, First Stage	8.66	8.80
Vertical Magnification, Second Stage	1.0	1.0
Vertical Magnification, Second Stage	0.09	0.06
K- $\pi$ Separation at Slit 1 (inches)	0.25(1200MeV/c)	0.11 (1600 MeV/c)
K- $\pi$ Separation at Slit 2 (inches)	0.28(1200MeV/c)	0.12 (1600MeV/c)

Table III

Physical Parameters of 20 BeV Spectrometer with a  
100 microsteradian Solid Angle and  $\pm 2\%$   
Momentum Bite

	Field gradient (Kg/cm)	Field (g)	Length (meters)	Aperture (approximate)
$Q_1$	0.385	-	2	$\pm 5$ cm
$Q_2$	0.466	-	2	$\pm 12$ cm
$M_1$	-	14.600	6	14 cm gap;
$Q_3$	0.410	-	2	$\pm 20$ cm
$M_2$	-	14.600	6	18 cm Gap 40 cm width



## References

1. Proc. Intern. Conf. on Instrumentation for High Energy Phys, Geneva, 1962, Notth-Holl, Publ. 1963.
2. Intern. Conf. on High Energy Accelerators. Dubna. 1963.
3. O.A. Valdner et al "Wave-Guide Particle Separation Methods" (submitted to the conference, but not published).
4. J.J. Murray et al. "A separated 2.5 to 2.8 GeV/c  $K^-$  beam at the Bevatron"
6. А.С.Вовенко и др. "Сепарированный пучок  $K^+$  мезонов с импульсом 20 ГэВ/с"
7. R. Ammar et al. "Status of the High-Momentum Mass-Separated Beam at the ZGS"
8. G. Brautti et al. "A high intensity enriched beam of kaons and antiprotons"
9. В.В.Владемирский, Е.К.Тарасов. "Применение магнитного зеркала для формирования нейтринного пучка"
10. W.K.H. Panofsky et al "A high-resolution production angle independently"
11. Joseph Ballam and Zoven G.T. Guiragossian "Almost Monochromatic photon beams at the Stanford Linear Accelerator Center"
12. К.Д.Толстов. "Мишень - водородная струя".
13. L.W. Jones "The Random Beam Optics"

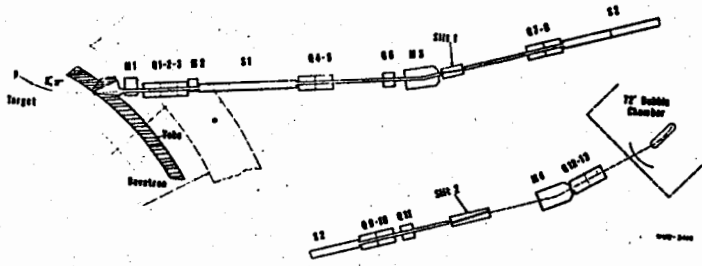


Fig.1. Schematic layout of K-63 beam apparatus.

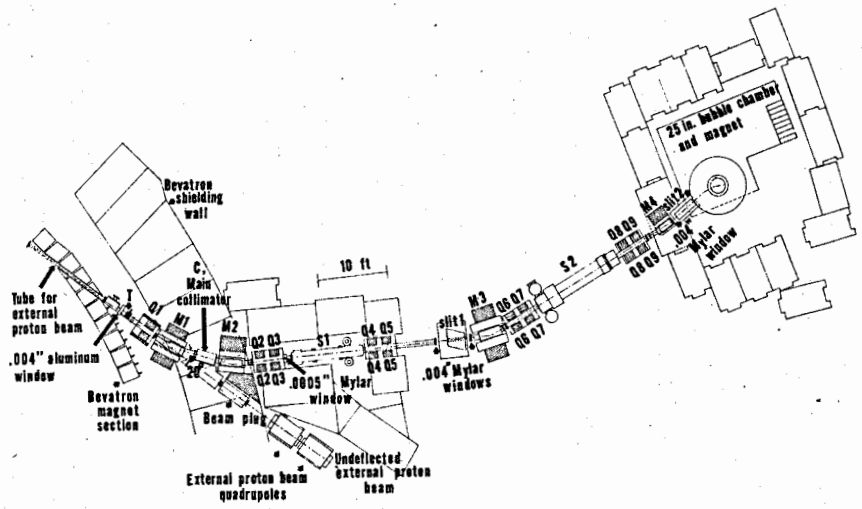


Fig.2. Plan view of layout of variable momentum K<sup>+</sup> beam.

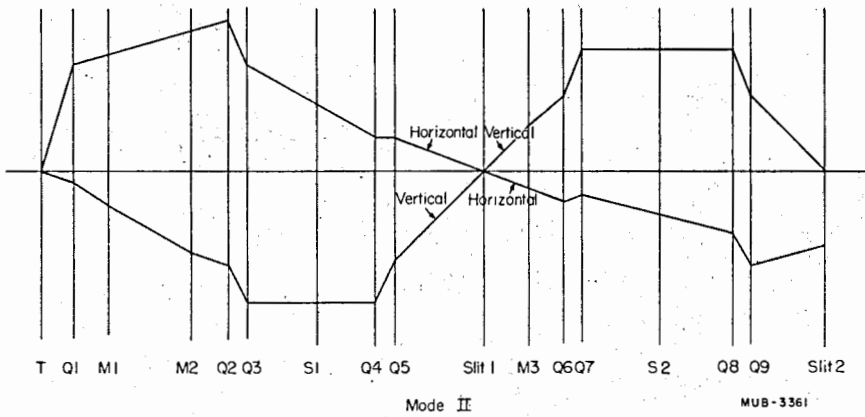
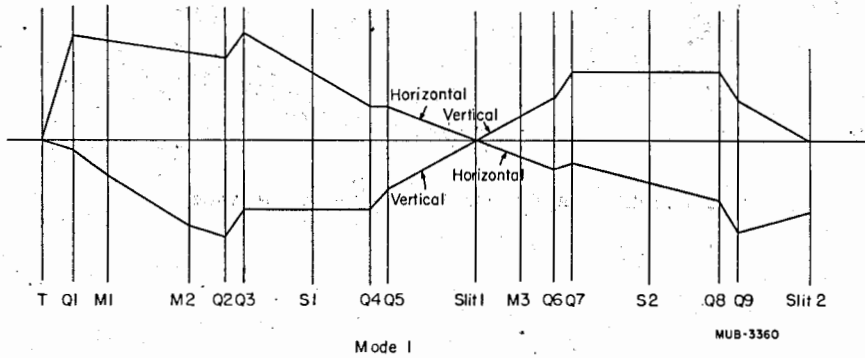


Fig. 3. Ray diagrams in the horizontal and vertical plane for Mode I and Mode II operation of the beam.

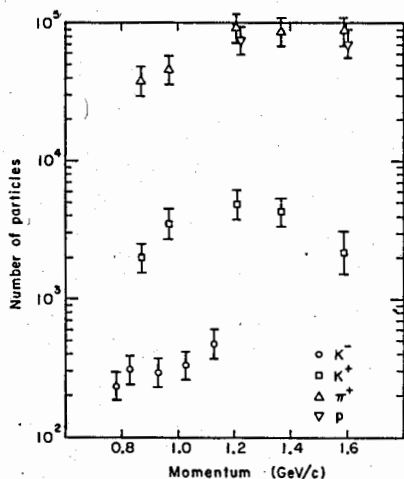


Fig.4. Secondary particle fluxes produced at  $0^\circ$  by 6 BeV protons, as function of momentum. The ordinate represents the number of particles per  $10^{11}$  protons in EPB channel, per 1% total momentum interval, per milliradian.

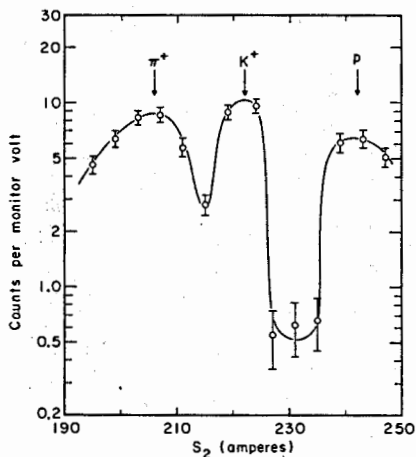


Fig.5. Separation curve at 1600 MeV/c beam momentum taken with the solid angle state counter at the second slit (Mcde II). Counts per monitor volts are plotted against the magnet current in the second spectrometer.

Схема K<sup>+</sup> пучкового канала на 2 ГэВ/с

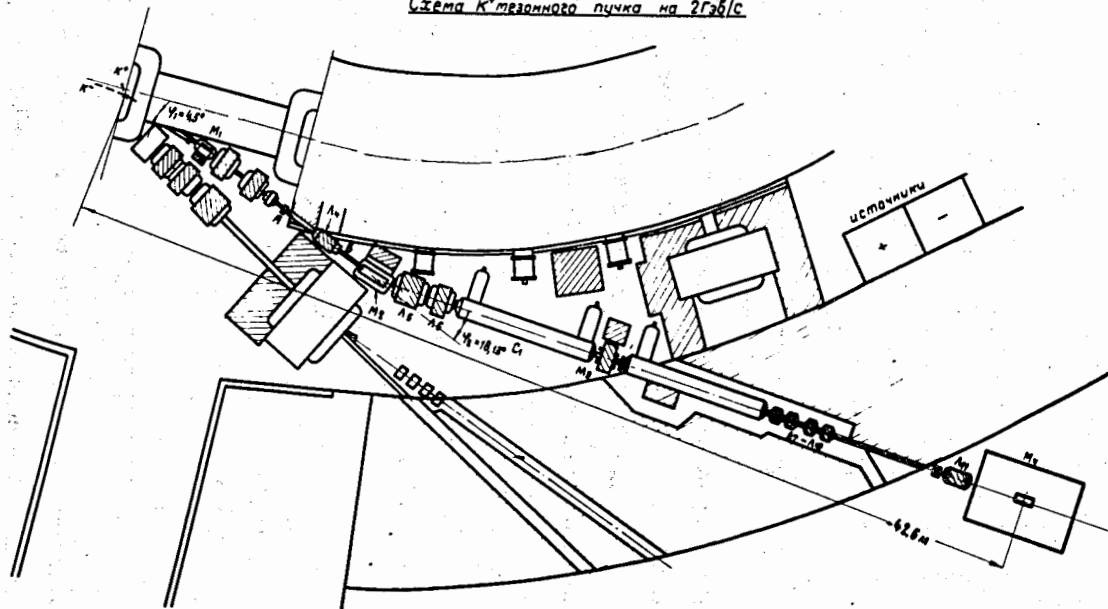


Fig.6. Schematic beam layout of 2.0 GeV/c K<sup>+</sup> beam.

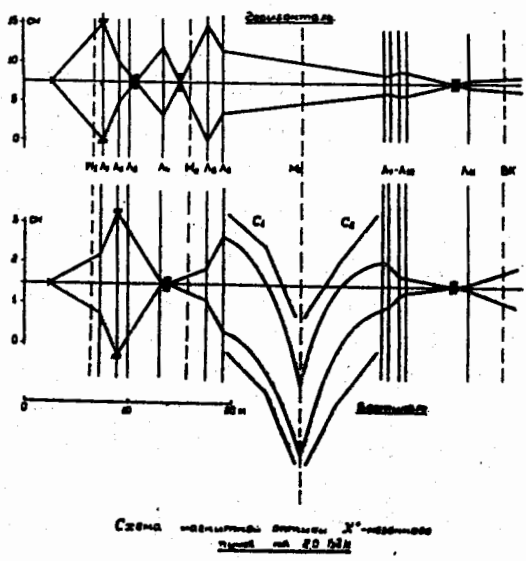
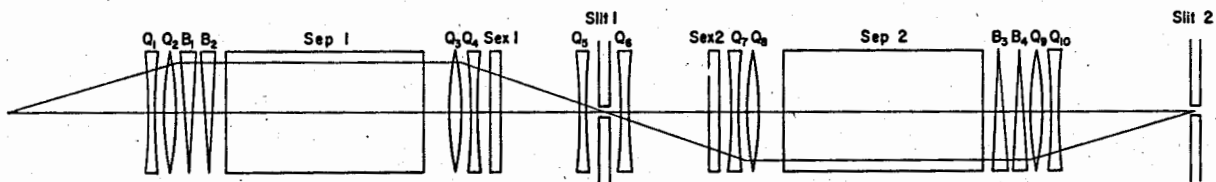
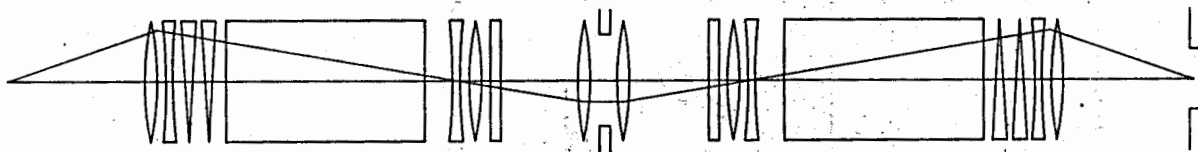


Fig.7. Ray diagrams for horizontal and vertical plane for 2.0 GeV/c K<sup>+</sup> beam.

VERTICAL MOTION



HORIZONTAL MOTION (IMAGING OF TARGET)



HORIZONTAL MOTION FOR CENTRAL RAYS OF DIFFERENT MOMENTA

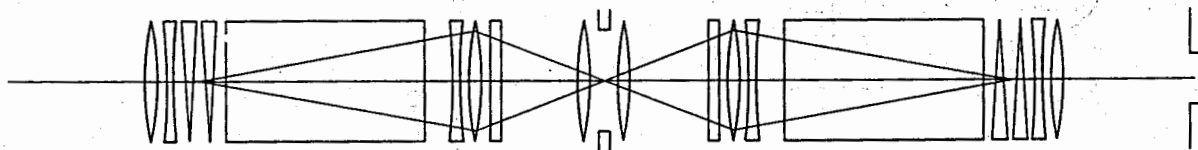


Fig.8. General pattern of optical design of mass-separated beam at ZGS.

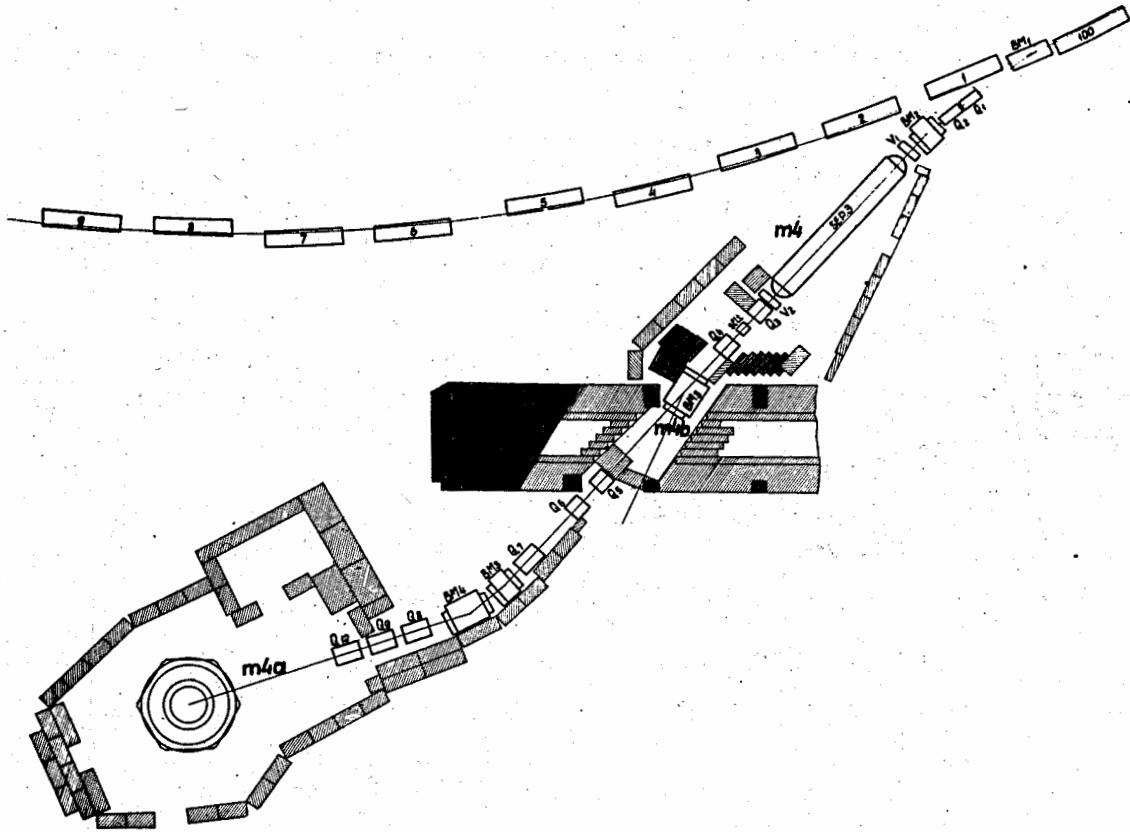


Fig.9. Schematic layout of high intensity enriched beam at CERN.



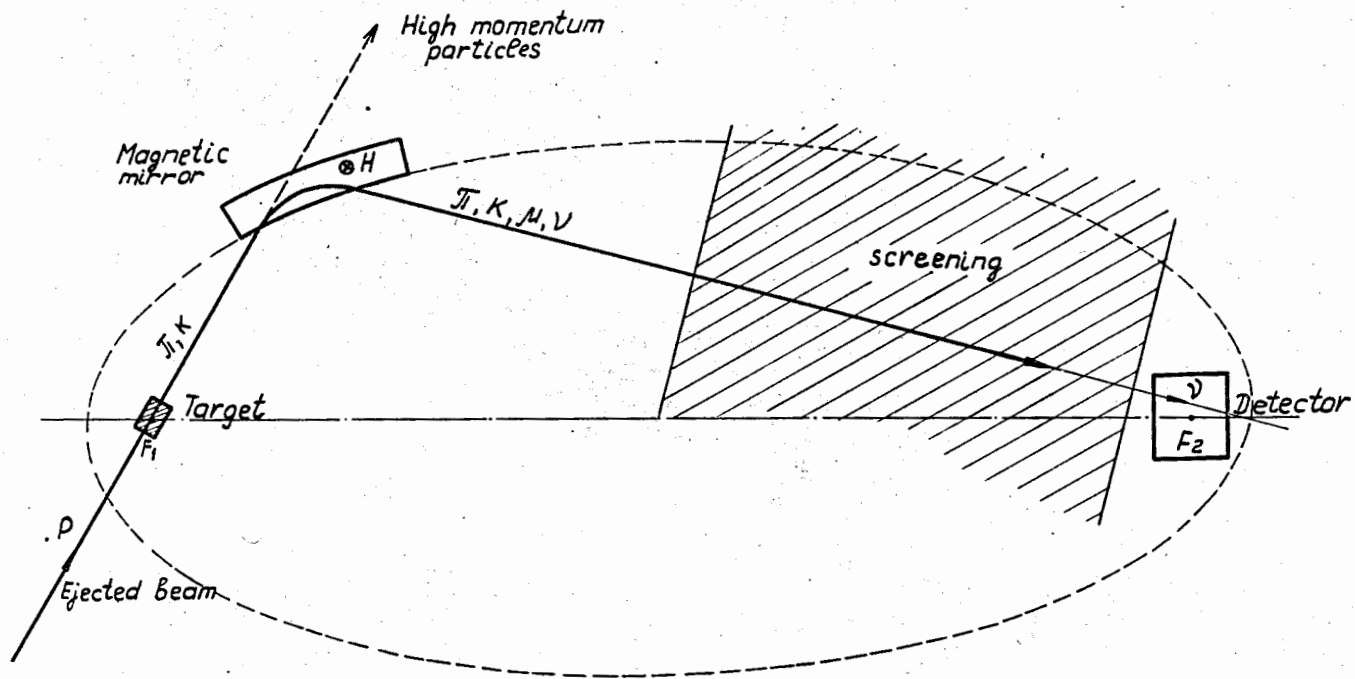


Fig.10. Scheme of ellipsoidal magnetic mirror for  $\nu$ -beam forming.

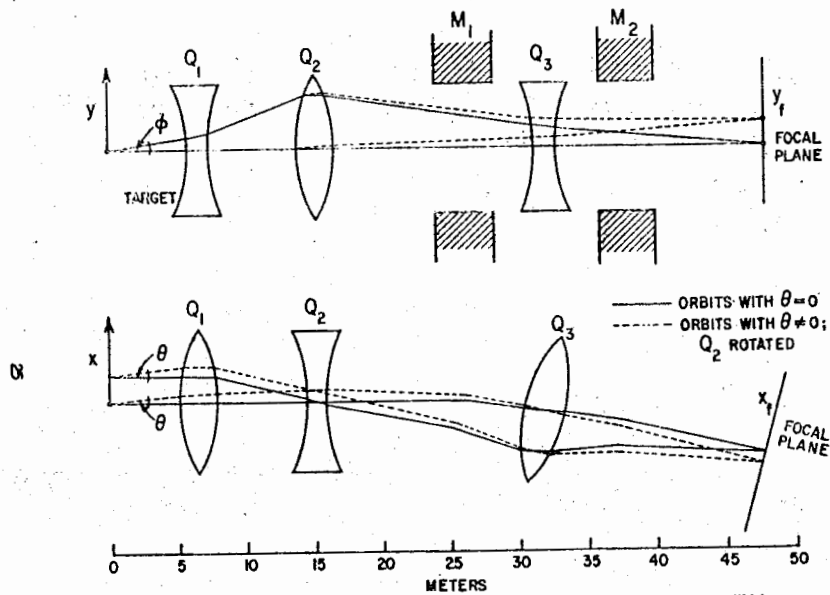


Fig.11. Ray diagrams for Magnetic spectrometer with rotated lens ( $Q_2$ ) and with vertical bending magnet respectively.

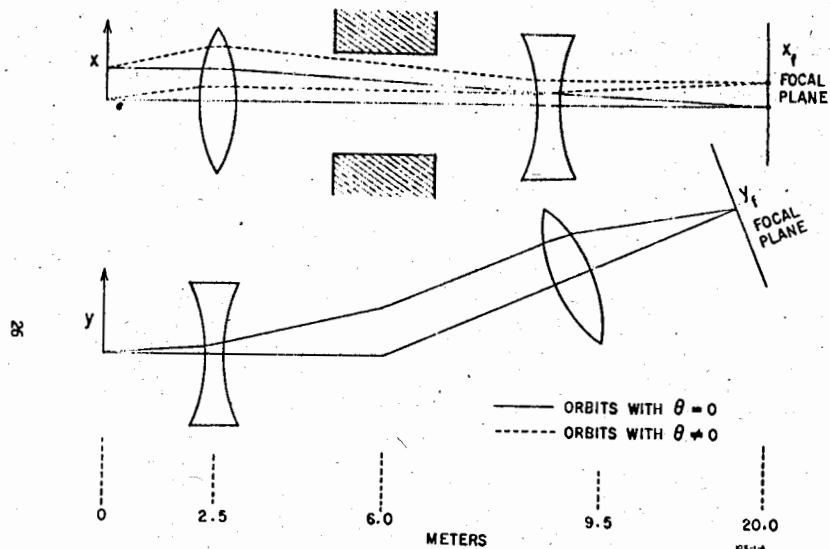


Fig.12. Ray diagrams for Magnetic spectrometer with rotated lens ( $Q_2$ ) and with vertical bending magnet respectively.

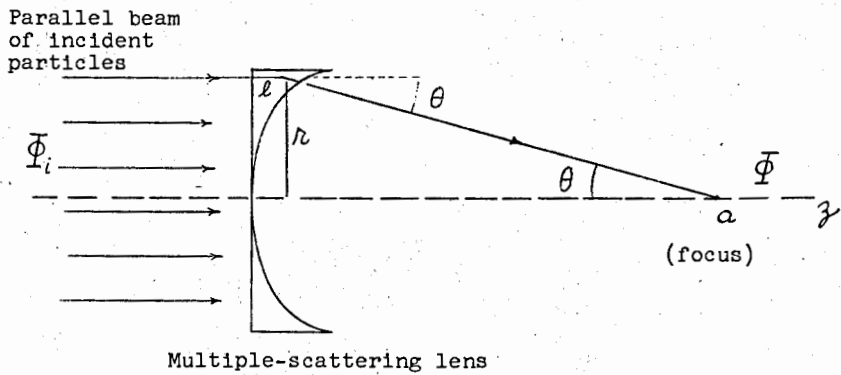
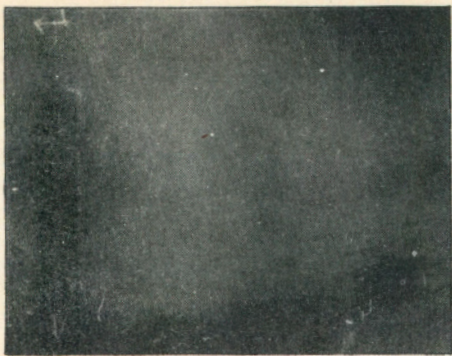
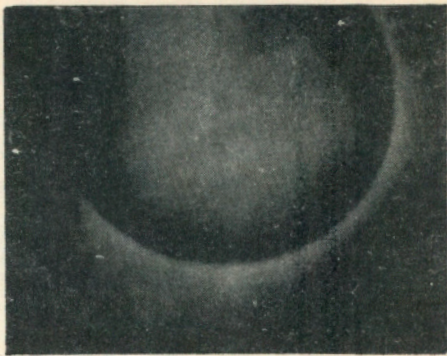


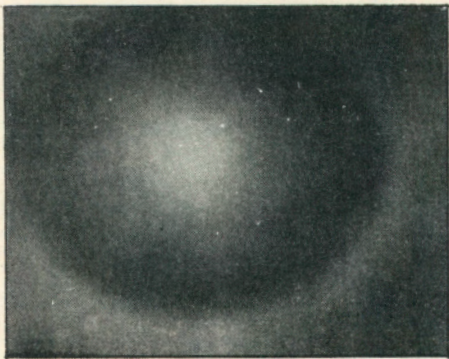
Fig.13. The geometry of a parabolic multiple-scattering lens.



a)



b)



c)

Figure 14. Polaroid films exposed to  $7 \times 10^9$  protons. a) "Parallel" beam with no lens. b) Image 35 inches beyond lead lens. c) Image 119 inches beyond lead lens (at the focus).